

## Short communication

Structural and microstructural characterization of  $\text{SiB}_{0.5}\text{C}_{1.5}\text{N}_{0.8}\text{Al}_{0.3}$  powders prepared by mechanical alloying using aluminum nitride as aluminum sourceDan Ye, De-Chang Jia<sup>\*</sup>, Zhi-Hua Yang, Xiao-Ming Duan, Yu Zhou*Institute for Advanced Ceramics, Harbin Institute of Technology, Harbin 150080, China*

Received 24 February 2011; received in revised form 24 March 2011; accepted 24 March 2011

Available online 5 April 2011

**Abstract**

$\text{SiB}_{0.5}\text{C}_{1.5}\text{N}_{0.8}\text{Al}_{0.3}$  powders were fabricated by mechanical alloying using crystalline silicon (c-Si), hexagonal boron nitride (h-BN), graphite (C) and aluminum nitride (AlN) powders as starting materials. The microstructure of the synthesized  $\text{SiB}_{0.5}\text{C}_{1.5}\text{N}_{0.8}\text{Al}_{0.3}$  powders is predominantly amorphous with a very small volume fraction of AlN nano-crystalline phase. The  $\text{SiB}_{0.5}\text{C}_{1.5}\text{N}_{0.8}\text{Al}_{0.3}$  powders appeared to possess a structure containing hybridization of several bonds such as Si–C, B–C–N, C–C, B–N and Al–N because of the solid reactions among c-Si, h-BN, graphite and AlN.  $^{29}\text{Si}$  and  $^{27}\text{Al}$  solid-state nuclear magnetic resonance spectra showed the formation of amorphous SiC structure based on  $\text{SiC}_4$  sites and the coexistence of  $\text{AlN}_4$  and  $\text{AlN}_5$  units in  $\text{SiB}_{0.5}\text{C}_{1.5}\text{N}_{0.8}\text{Al}_{0.3}$  powders, respectively.

© 2011 Elsevier Ltd and Techna Group S.r.l. All rights reserved.

**Keywords:** A. Powders; solid state reaction; A. Milling; B. Electron microscopy;  $\text{SiB}_{0.5}\text{C}_{1.5}\text{N}_{0.8}\text{Al}_{0.3}$  powders**1. Introduction**

SiBCN ceramics derived from polymer precursor have attracted a lot of attention for high-temperature structural applications due to their excellent high-temperature stability [1], high oxidation resistance [2] and mechanical properties [3]. However, oxidation at 1500 °C for 24 h resulted in crystallisation of the formerly amorphous oxide scales with concurrent bubble formation because of volatilisation of boron species [4]. In order to improve the quality of the oxide scales, thereby improving oxidation resistance, Müller et al. introduced aluminum into the system and prepared a new kind of SiBCNAl precursor-derived ceramics [5]. It was found that the addition of aluminum indeed played a beneficial role in the inhibition of bubble formation as well as cracking and spallation of the oxide scales.

The ceramics fabricated by the pyrolysis of polymer precursors show high purity and homogeneous elemental distribution. But the synthesis and pyrolysis of precursors need to be done in inert gases, and the corresponding processes are

very complicated and most transforming processes from polymer precursors to dense bulk ceramics are always combined with decomposition reactions, so the development of new synthesis routes for SiBCNAl powders and ceramics is necessary. Ball-milling-induced solid-state amorphization (SSA, or crystalline-to-amorphous phase transformation) recently has received significant attention because the combination of ball milling and subsequent consolidation may offer a way to produce technologically useful bulk amorphous materials [6]. Solid-state amorphization by mechanical alloying (MA) involves repeated welding, fragmentation and rewelding of powder particles in a high-energy ball mill. MA has now been shown to be capable of synthesizing a variety of equilibrium and non-equilibrium alloy phases starting from blended elemental or prealloyed powders [6].

In our previous work, amorphous  $\text{SiB}_{0.5}\text{C}_{1.5}\text{N}_{0.5}\text{Al}_{0.3}$  powders have been fabricated by MA using c-Si, h-BN, graphite and aluminum (Al) powders as starting materials [7]. In order to further investigate the influence of different aluminum source on the microstructure and structure of SiBCNAl powders, we prepared  $\text{SiB}_{0.5}\text{C}_{1.5}\text{N}_{0.8}\text{Al}_{0.3}$  powders using AlN powder as the source of aluminum in this paper for the first time.

<sup>\*</sup> Corresponding author. Tel.: +86 451 86418792; fax: +86 451 86414291.

E-mail address: [dchjia@yahoo.com.cn](mailto:dchjia@yahoo.com.cn) (D.-C. Jia).

## 2. Experimental

Commercially available crystalline silicon (c-Si, ca. 15  $\mu\text{m}$ , >99.5% pure, Beijing, China), hexagonal boron nitride (h-BN, ca. 0.6  $\mu\text{m}$ , >98% pure, Beijing, China), graphite (C, ca. 4  $\mu\text{m}$ , >99.9% pure, Qingdao, China) and aluminum nitride (AlN, ca. 0.5  $\mu\text{m}$ , >98.5% pure, Beijing, China) powders were blended in mole ratio of Si:BN:C:AlN = 1:0.5:1.5:0.3 to give a composition of  $\text{SiB}_{0.5}\text{C}_{1.5}\text{N}_{0.8}\text{Al}_{0.3}$  and then mechanically alloyed in a high-energy planetary ball mill (Fritsch Pulverisette 4, Germany) using silicon nitride ( $\text{Si}_3\text{N}_4$ ) vials and silicon nitride balls (10 mm in diameter). Transferring the powders into and from the vials was carried out in a glove box filled with pure (99.99%) argon.

Phase structures of as-prepared powders were examined using X-ray diffraction (XRD) methods with Cu  $K\alpha$  radiation. Particle morphology observation was performed on a Tecnai F30 field emission gun transmission electron microscope (TEM). High-resolution transmission electron microscopy (HRTEM) studies were carried out using a Tecnai F30 TEM instrument operated at 300 kV. The X-ray photoelectron spectroscopy (XPS) analysis was performed on a PHI ESCA system using Al  $K\alpha$  radiation ( $h\nu = 1486.6 \text{ eV}$ ). The signal curves were fitted by deconvolutions of peaks using Gaussian–Lorentzian peak approximations and Shirley background reduction.  $^{29}\text{Si}$  and  $^{27}\text{Al}$  solid-state magic angle spinning (MAS) nuclear magnetic resonance (NMR) spectra were

recorded on a Bruker Avance III 400 spectrometer, operating at 79.3 MHz for Si and 104 MHz for Al.

## 3. Results and discussion

A set of experiments with different milling times and ball-to-powder mass ratio (B/P) were conducted in order to prepare amorphous  $\text{SiB}_{0.5}\text{C}_{1.5}\text{N}_{0.8}\text{Al}_{0.3}$  powders. Fig. 1(a) shows the XRD patterns of the powder mixture milled with a B/P of 30:1 for different milling times. It is shown that the diffraction peaks of AlN can still be observed after 30 h of milling. This indicates that amorphization of the powder mixture using AlN powder as aluminum source is more difficult than that of the sample using Al powder as aluminum source [7]. When the milling time is up to 60 h, the powders are still not completely amorphous with very small diffraction peaks of AlN. Next the milling time was maintained at 30 h with different B/P (as shown in Fig. 1(b)). These XRD patterns indicate that the milling efficiency is enhanced as the B/P increases. When the B/P is increased to 50:1, a halo peak corresponding to an amorphous phase is observed and the sample can be considered as completely X-ray amorphous. In the following experiments, the  $\text{SiB}_{0.5}\text{C}_{1.5}\text{N}_{0.8}\text{Al}_{0.3}$  powders which were milled for 30 h with a B/P of 50:1 were studied.

Fig. 2(a) gives the TEM image of  $\text{SiB}_{0.5}\text{C}_{1.5}\text{N}_{0.8}\text{Al}_{0.3}$  powder particles. As shown, the powder particle sizes are about 100–200 nm with some agglomerated particles. A typical

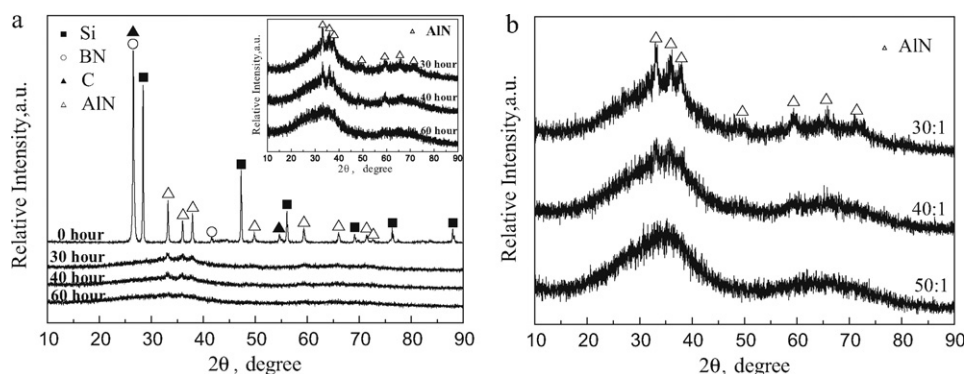


Fig. 1. XRD patterns of the powder mixture milled for (a) different times with a B/P of 30:1 and (b) 30 h with different B/P. The inset in (a) is the enlarged XRD patterns of the powder mixture milled for 30, 40 and 60 h.

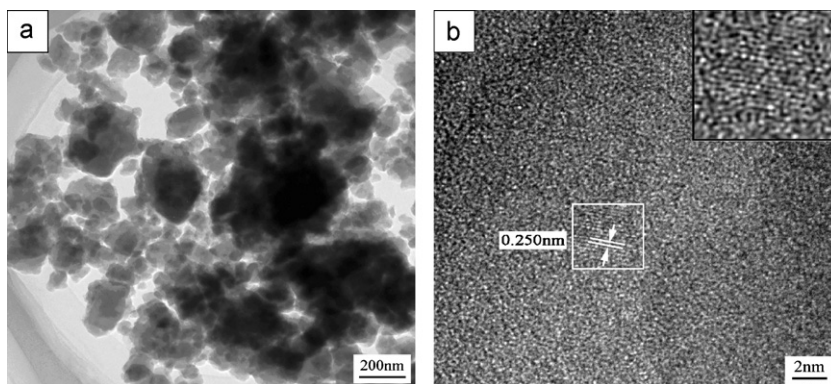


Fig. 2. (a) TEM and (b) HRTEM images of  $\text{SiB}_{0.5}\text{C}_{1.5}\text{N}_{0.8}\text{Al}_{0.3}$  powder particles. The inset in (b) is the inverse FFT image of the area marked by the white square.

HRTEM image of the powder particles is shown in Fig. 2(b). It is evident that the microstructure of the powders is predominantly amorphous with a very small volume fraction of nano-crystalline phase (as shown in the area marked by the white square in Fig. 2(b)). The interplanar distance measured from the image is  $0.250 \pm 0.002$  nm, which matches well with  $d(1\ 1\ 1) = 0.251$  nm of  $\beta$ -SiC (3C) or  $d(0\ 0\ 2) = 0.251$  nm of AlN. In view of previous studies which did not find the existence of  $\beta$ -SiC nano-crystalline under the similar milling conditions [7], the nano-crystalline phase in Fig. 2(b) can be identified as AlN crystalline. The reason for incomplete amorphization of AlN may be that it is more difficult to break the Al–N bonds with larger bond energy than the other bonds involved. The inverse fast Fourier transform (FFT) image of the area marked by the white square shows that distorted regions are formed in the AlN nano-crystalline particle (as shown in the inset of Fig. 2(b)).

In order to investigate the bonding state of the as-prepared  $\text{SiB}_{0.5}\text{C}_{1.5}\text{N}_{0.8}\text{Al}_{0.3}$  powders, XPS analysis was carried out. Table 1 gives the deconvolution results of the corresponding chemical binding state of each element in the  $\text{SiB}_{0.5}\text{C}_{1.5}\text{N}_{0.8}\text{Al}_{0.3}$  powders. The results revealed that the solid reactions among c-Si, h-BN, graphite and AlN occurred by MA, which resulted in the generation of new chemical bonds. Compared with the  $\text{SiB}_{0.5}\text{C}_{1.5}\text{N}_{0.5}\text{Al}_{0.3}$  powders prepared using Al powder as the source of aluminum [7], the  $\text{SiB}_{0.5}\text{C}_{1.5}\text{N}_{0.8}\text{Al}_{0.3}$  powders have similar bonding types but no oxygen-containing bonds.

$^{29}\text{Si}$  and  $^{27}\text{Al}$  solid-state NMR spectra of the  $\text{SiB}_{0.5}\text{C}_{1.5}\text{N}_{0.8}\text{Al}_{0.3}$  powders are shown in Fig. 3. The broad peak at  $-18.3$  ppm (as shown in Fig. 3(a)) indicates that amorphous

Table 1

Deconvolution results of the corresponding chemical binding state of each element in the  $\text{SiB}_{0.5}\text{C}_{1.5}\text{N}_{0.8}\text{Al}_{0.3}$  powders.

Element line	Bonding type	$E_B$ (eV)
Si2p	Si–C	101.0 [8]
B1s	B–N	189.4 [9]
	B–C–N	192.1 [9]
C1s	C–Si	282.7 [8]
	C–C	284.7 [9]
	C–B–N	285.8 [9]
	N–Al	397.0 [10]
N1s	N–B	398.1 [9]
	N–B–C	400.9 [9]
	Al–N	73.8 [11]

SiC structure based on  $\text{SiC}_4$  sites was formed in  $\text{SiB}_{0.5}\text{C}_{1.5}\text{N}_{0.8}\text{Al}_{0.3}$  powders [12]. A small peak at  $-90.3$  ppm is attributed to the residual starting Si material due to insufficient milling [12]. Fig. 3(b) and (c) show  $^{27}\text{Al}$  NMR spectra of the starting AlN and as-prepared  $\text{SiB}_{0.5}\text{C}_{1.5}\text{N}_{0.8}\text{Al}_{0.3}$  powders, respectively. The signal at 112.8 ppm suggests that the environment of aluminum atoms is tetrahedral  $\text{AlN}_4$  sites in the starting AlN powders (as shown in Fig. 3(b)) [13]. After milling, the  $^{27}\text{Al}$  chemical shifts of  $\text{SiB}_{0.5}\text{C}_{1.5}\text{N}_{0.8}\text{Al}_{0.3}$  powders are at 112.9 and 57.0 ppm corresponding to the  $\text{AlN}_4$  and  $\text{AlN}_5$  units, respectively (as shown in Fig. 3(c)) [13]. The result indicates that the local environment around the aluminum atoms changes from  $\text{AlN}_4$  to the mixture of  $\text{AlN}_4$  and  $\text{AlN}_5$  by mechanical alloying. As compared with the  $\text{SiB}_{0.5}\text{C}_{1.5}\text{N}_{0.5}\text{Al}_{0.3}$  powders prepared using Al powder as the source of aluminum [7], the

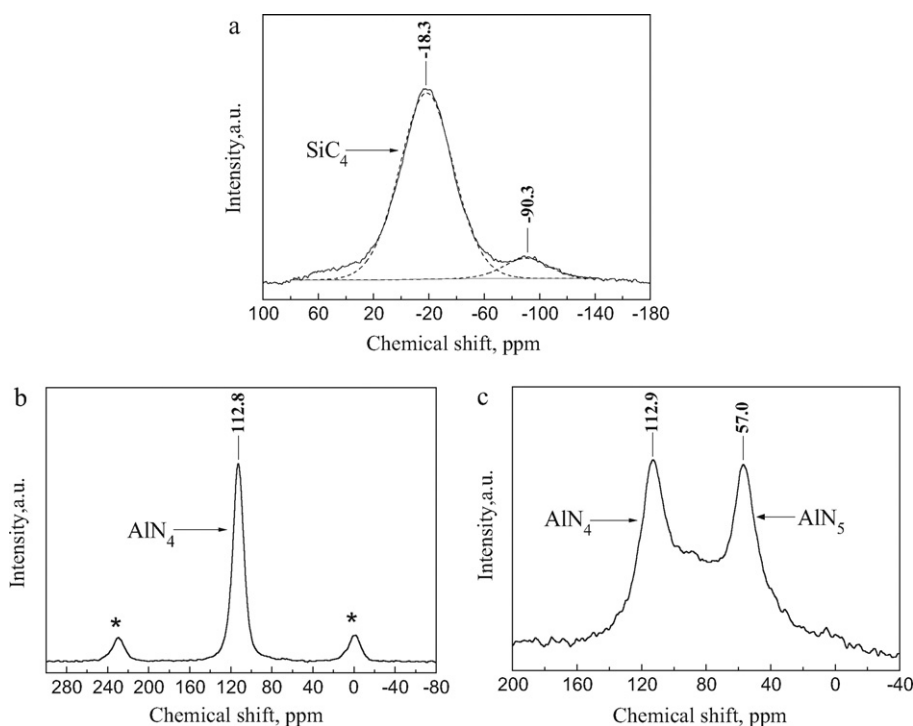


Fig. 3. (a)  $^{29}\text{Si}$  NMR spectrum of the  $\text{SiB}_{0.5}\text{C}_{1.5}\text{N}_{0.8}\text{Al}_{0.3}$  powders;  $^{27}\text{Al}$  NMR spectra of (b) the starting AlN and (c) as-prepared  $\text{SiB}_{0.5}\text{C}_{1.5}\text{N}_{0.8}\text{Al}_{0.3}$  powders. (Asterisks denote spinning sidebands.)

$\text{SiB}_{0.5}\text{C}_{1.5}\text{N}_{0.8}\text{Al}_{0.3}$  powders have relatively simple environment of aluminum atoms because it is more difficult to break the Al–N bonds of AlN powder than the Al–Al bonds of Al powder.

#### 4. Conclusions

The as-prepared  $\text{SiB}_{0.5}\text{C}_{1.5}\text{N}_{0.8}\text{Al}_{0.3}$  powders are predominantly amorphous with a very small volume fraction of AlN nano-crystalline phase. The solid reactions among c-Si, h-BN, graphite and AlN powders occurred and resulted in the generation of new chemical bonds. The environments of silicon and aluminum atoms are tetrahedral  $\text{SiC}_4$  sites and the mixture of  $\text{AlN}_4$  and  $\text{AlN}_5$  units, respectively. Compared with the  $\text{SiB}_{0.5}\text{C}_{1.5}\text{N}_{0.5}\text{Al}_{0.3}$  powders prepared using Al powder as the source of aluminum [7], the  $\text{SiB}_{0.5}\text{C}_{1.5}\text{N}_{0.8}\text{Al}_{0.3}$  powders are not completely amorphous, possess similar bonding types but no oxygen-containing bonds and have relatively simple environment of aluminum atoms under the milling conditions used in this paper.

#### References

- [1] R. Riedel, A. Kienzle, W. Dressler, L. Ruwisch, J. Bill, F. Aldinger, A silicoboron carbonitride ceramic stable to 2000 °C, *Nature* 382 (1996) 796–798.
- [2] H.P. Baldus, M. Jansen, Novel high-performance ceramics—amorphous inorganic networks from molecular precursors, *Angew. Chem. Int. Ed. Engl.* 36 (1997) 328–343.
- [3] R. Riedel, L.M. Ruswisch, L. An, R. Raj, Amorphous siliconboron carbonitride ceramic with very high viscosity at temperatures above 1500 °C, *J. Am. Ceram. Soc.* 81 (1998) 3341–3344.
- [4] E. Butchereit, K.G. Nickel, A. Müller, Precursor-derived Si–B–C–N ceramics: oxidation kinetics, *J. Am. Ceram. Soc.* 84 (2001) 2184–2188.
- [5] A. Müller, P. Gerstel, E. Butchereit, K.G. Nickel, F. Aldinger, Si/B/C/N/Al precursor-derived ceramics: Synthesis, high temperature behaviour and oxidation resistance, *J. Eur. Ceram. Soc.* 24 (2004) 3409–3417.
- [6] C. Suryanarayana, Mechanical alloying and milling, *Prog. Mater. Sci.* 46 (2001) 1–184.
- [7] D. Ye, D.C. Jia, Z.H. Yang, Z.L. Sun, P.F. Zhang, Microstructure and thermal stability of amorphous SiBCNAl powders fabricated by mechanical alloying, *J. Alloys Compd.* 506 (2010) 88–92.
- [8] W.F.A. Besling, A. Goossens, B. Meester, J. Schoonman, Laser-induced chemical vapor deposition of nanostructured silicon carbonitride thin films, *J. Appl. Phys.* 83 (1998) 544–553.
- [9] Y.H. Xiong, C.S. Xiong, S.Q. Wei, H.W. Yang, Y.T. Mai, W. Xu, S. Yang, G.H. Dai, S.J. Song, J. Xiong, Z.M. Ren, J. Zhang, H.L. Pi, Z.C. Xia, S.L. Yuan, Study on the bonding state for carbon-boron nitrogen with different ball milling time, *Appl. Surf. Sci.* 253 (2006) 2515–2521.
- [10] R. Dalmau, R. Collazo, S. Mita, Z. Sitar, X-ray photoelectron spectroscopy characterization of aluminum nitride surface oxides: thermal and hydrothermal evolution, *J. Electron. Mater.* 36 (2007) 414–419.
- [11] N. Duez, B. Mutel, C. Vivien, L. Gengembre, P. Goudmand, O. Dessaux, J. Grimblot, XPS investigation of aluminum and silicon surfaces nitrided by a distributed electron cyclotron resonance nitrogen plasma, *Surf. Sci.* 482/485 (2001) 220–226.
- [12] S. Harrison, X.Q. Xie, K.J. Jakubenas, H.L. Marcus, Silicon-29 solid-state MAS NMR investigation of selective area laser deposition silicon carbide material, *J. Am. Ceram. Soc.* 82 (1999) 3221–3224.
- [13] R. Toyoda, S. Kitaoka, Y. Sugahara, Modification of perhydropolysilazane with aluminum hydride: preparation of poly(aluminasilazane)s and their conversion into Si–Al–N–C ceramics, *J. Eur. Ceram. Soc.* 28 (2008) 271–277.